Article

Smart polymer functionalized graphene nano-devices for thermo-switch controlled biodetection

Mustafa Balcioglu, Burak Zafer Buyukbekar, Mustafa Selman Yavuz, and Mehmet Veysel Yigit

ACS Biomater. Sci. Eng., **Just Accepted Manuscript** • Publication Date (Web): 21 Nov 2014

Smart polymer functionalized graphene nano-devices for thermo-switch controlled biodetection

Mustafa Balcioglu[†], Burak Zafer Buyukbekar[‡], Mustafa Selman Yavuz[‡], and Mehmet V. Yigit [†, *]

†Department of Chemistry and RNA Institute,
University at Albany, State University of New York,
1400 Washington Avenue, Albany, New York 12222, United States

and

‡Department of Metallurgy and Materials Engineering,
Advanced Technology Research and Application Center,
Selcuk University, Konya, Turkey

*Correspondence:
Mehmet V. Yigit
Tel: (1) 518-442-3002
myigit@albany.edu

Abstract

In this work, we have developed a general methodology for constructing an activatable biosensor utilizing a thermo-responsive polymer and two-dimensional nano-sheet. We have demonstrated the detection of four different types of biological compounds using the smart PEGMA (poly(ethylene glycol) methyl ether methacrylate), oligonucleotides and graphene oxide nano-assembly. The activity of the functional nano-device is controlled with a thermo-switch at 39 °C. In this design, the nano-sized graphene oxide serves as a template for fluorophore labeled probe oligonucleotides while quenching the fluorescence intensities dramatically. On the other hand, the PEGMA polymer serves as an activatable protecting layer covering the graphene oxide and entrapping the probe oligonucleotides on the surface. The PEGMA polymers are hydrophobic above their **l**ower **c**ritical **s**olution **t**emperature (LCST) and therefore interact strongly with the hydrophobic surface of graphene oxide, creating a closed configuration (OFF state) of the nano-device. However, once the temperature decreases below the LCST, the polymer undergoes conformational change and becomes hydrophilic. This opens up the surface of the graphene oxide (open configuration, ON state), freeing the encapsulated payload on the surface. We have tuned the activity of the nano-device for the detection of a sequence specific DNA, *miR*-10b, thrombin and adenosine. The activity of our functional system can be decreased by ~80% with a thermo-switch at 39 °C. Our approach can be extended to other anti-sense oligonucleotide, aptamer or DNAzyme based sensing strategies.

Keywords: nano-device, graphene, thermo-responsive polymer, PEGMA, DNA, miRNA, thrombin, adenosine, aptamer.

Introduction

Engineering smart stimuli-responsive nano-devices has been an important goal for many biological and environmental applications. Controlling the function of the nano-assemblies enables researchers to activate the detection of the target molecules, or delivery and release of the therapeutic cargo, to the tissue of interest only when spatial/temporal activity is needed. [1-9] Such an approach provides precise control over the activity of the functional material with minimum off-target effect and background signals. Moreover, it protects the valuable payload in the nano-assemblies from degrading or leaking. Thermo-responsive polymers are superb candidates for constructing activatable functional nanomaterials.[4, 10-12] These polymers undergo a dramatic conformational change with external stimuli which creates a remarkable change in their environment.[13-14] Due to their predictable and controllable features they have been investigated for designing devices which can be switched on and off with external input.[2] Smart polymer based assemblies have a stimuli-induced response, which takes advantage of the unique conformational changes as a function of temperature,[15-16] pH,[17-21] ionic strength,[22] electric or magnetic field,[23-26] light[27-30] and/or chemical and biological stimuli.[31-32] Interest in stimuli-responsive polymers has persisted over many decades and a great deal of work has been dedicated for developing environmentally-sensitive macromolecules that can be constructed into new smart materials. For example, it was shown that thermo-responsive polymer functionalized gold nano-cages can release the encapsulated drug payload with a thermal switch, which enabled the authors to control the efficacy of chemotherapy on cancer cell lines.[2] Recently, Maye and coworkers modified DNA-capped gold nanoparticles with thermo-responsive smart (pNIPAAm-co-pAAm) polymers for regulating a DNA-encoded drug delivery system.[5] In both of these studies thermo-responsive polymers undergo conformational changes enabling the accessibility

of the encapsulated materials. We have used thermo-responsive PEGMA (poly(ethylene glycol) methyl ether methacrylate) polymer in our studies which undergoes a conformational change at the **l**ower **c**ritical **s**olution **t**emperature (LCST).[15, 33] The PEGMA polymer is hydrophobic at temperatures above the LCST, however once the temperature decreases below the LCST, the polymer undergoes a transition and becomes hydrophilic.[15, 34] Such a response to external physical conditions holds great potential for designing activatable and functional devices by conjugation of PEGMA to nanostructures, such as graphene oxide.

Graphene oxide (GO) is an atomically thin two-dimensional carbon material with unique electrical, thermal, and mechanical properties.[35-36] It has arisen as a superb template for tracing numerous biological processes due to its extraordinary physical properties at the bio-nano interfaces.[37-38] It also has a large surface area and good water dispersibility which makes it practical for sensing and biomedical applications.[39-40] GO has a remarkable single-stranded DNA (ssDNA) adsorption capacity due to the specific chemical interactions between its surface and the nucleobases of the oligonucleotides.[41] However, in the presence of complementary oligonucleotides or DNA binding molecules, the surface-adsorbed ssDNA molecules are released from the surface due to target recognition.[42] This reversible interaction has been used as the primary tool for utilizing GO as a potent platform for various biological and environmental applications.[43] Furthermore, due to its powerful fluorescence quenching capability, the fluorescence of molecular dye labeled DNA molecules on GO surface can be quenched almost completely. However, upon release of the DNAs from the surface the fluorescence recovery is observed as a function of target concentration and time.[44] The fluorescence quenching capacity and the reversible oligonucleotide adsorption and desorption properties make GO a promising nanomaterial for biosensing approaches.[45]

Since GO has such powerful features as a sensing and theranostic material, engineering an activatable nano-device using GO and smart polymers could advance its applications and minimize the drawbacks, significantly. Graphene oxide can be prepared in nanoscale (nGO) size with several carboxyl terminals at the edges, which enables conjugation of polymers and biocompounds, such as DNAs.[44-47] Here, we have used these edges as conjugation sites for carboxyl-terminated thermo-responsive PEGMA polymers to nGO through a covalent amide linkage. The nGO was first aminated with the introduction of the amine (NH_2) groups of ethylenediamine via the (EDC)-mediated coupling reaction.[48] The carboxyl modified polymers were later conjugated to the aminated nGOs through amide linkages.[45, 47] The purified nGO-PEGMA was used for detection of a DNA, oncomiR, protein and metabolite using anti-sense oligonucleotides or aptamers and its the retention strength was examined under different temperatures. Aptamers in this study serve as functional oligonucleotides which undergo structural switching upon target recognition.[49] The working scheme of our system is based on the fact that PEGMA polymers are hydrophobic above their LCST and lay tightly on the hydrophobic surface of nGO, creating a closed configuration of the device and entrapping the surface adsorbed probe DNA strands. However, once the temperature decreases below the LCST, the polymer undergoes conformational change and becomes hydrophilic.[14-15] This opens up the surface of the nGO, freeing the encapsulated payload on the surface. We have utilized this system for the detection of several biocompounds and controlled its activity with a thermo-switch at 39 °C. Even though we have only tested a short ssDNA, miRNA, protein and small metabolite, this approach can be generalized for other detection schemes and target molecules. We believe that the temperature-controlled biodetection approach could be important for biomedical applications, particularly for noninvasive detection or targeting medically important

bio-compounds only at the tissue of interest with a change in temperature induced by laser irradiation.[2]

Experimental Section

Materials. All DNA sequences were purchased from Integrated DNA Technologies (IDT) (Coralville, IA) with following sequence information and modifications,

(1) FAM-labeled probe DNA (P1) 5'-/FAM/TACCCTGTAGAACCGAATTTGTG-3',

(2) complementary target DNA sequence (C1) 5'-CACAAATTCGGTTCTACAGGGTA-3',

(3) non-complementary DNA sequence (nC1) 5'-TACCCTGTAGAACCGAATTTGTG-3',

(4) miR-10b RNA 5'-UACCCUGUAGAACCGAAUUUGUG-3'

(5) anti-sense miR-10b DNA sequence (P1) 5'-/FAM/CACAAATTCGGTTCTACAGGGTA-3',

(4) Adenosine aptamer, 5'-/FAM/ACCTGGGGGAGTATTGCGGAGGAAGGT-3',

(5) Thrombin aptamer, 5'-/FAM/AGTCCGTGGTAGGGCAGGTTGGGGTGACT-3'.

Carboxyl graphene water dispersion was purchased from ACS Material (Medford, MA). Oligo(ethylene glycol) metilethermethacrylate (OEGMA, Mn 500), Di(ethylene glycol) methyl ether methacrylate (DEGMA), 4,4′-Azobis(4-cyanovaleric acid) (ACVA, initiator) were purchased from Sigma-Aldrich and used as received. Methanol and dialysis tubing cellulose membrane (Fisherbrand, cut-off 12,000-14,000) were purchased for VWR and Fisher Scientific, respectively, and used as received. Adenosine, inosine, guanosine, cytidine, uridine were purchased from AMRESCO LLC (Solon, OH). Thymine was purchased from Alfa Aesar (Ward Hill, MA). Human α-thrombin (Catalog Number: HCT-0020) was purchased Haematologic Technologies, Inc. (Essex Junction, VT). Bovine serum albumin (BSA) and streptavidin (STA) were purchased from AMRESCO LLC (Solon, OH). All other reagents were purchased from

Sigma-Aldrich (St. Louis, MO) and used without further purification. Double distilled water was used in preparation of all solutions. RNAse-free water was used for RNA experiments.

Preparation of acid functionalized PEGMA [PEGMA-COOH] using Free Radical Polymerization. The LCST for the corresponding PEGMA polymer (45 kDa) was set to 39 °C (DEGMA:OEGMA, 90:10). In a typical synthesis, 0.657 g OEGMA (1.384 mmol), 2.35 g DEGMA (12.5 mmol), 11 mg ACVA (0.04 mmol), 6 mL distilled water and 4 mL methanol were mixed in a 20 mL Pyrex glass reactor. The mixture was magnetically stirred for 3 h at 70 °C under nitrogen flow. Once polymerization was complete, the reaction mixture was inserted into a dialysis tubing cellulose membrane and purified by dialysis at room temperature (RT).

Attachment of PEGMA to nGO. First, the nGO was aminated by reacting 5 ml of 240 μg/mL nGO suspension (final 220 μg/mL) with 300 mg EDC (final 54.5 mg/mL) and 250 μL of 0.9 mg/mL ethylenediamine (final 41 μg/mL) in 10 mM MES buffer (pH 5.2) for 12 hrs at RT. The resulting nGO suspension was dialyzed against DI water using 13 kDa MWCO dialysis bag to remove excess EDC and ethylenediamine. After the dialysis was complete, the sample was concentrated by centrifugation at 15000 rpm for 15 min and was redispersed in 4 mL of DI water to a final concentration of 220 μg/mL nGO. The amination yield was determined by attachment of SPDP (*N*-Succinimidyl 3-(2-pyridyldithio)-propionate, 50 μL of 10 mg/mL) to amine terminals of nGO (750 μL of 80 μg/mL) in PBS buffer pH 7.4 and quantification of released pyridine-2-thione (P2T, $\varepsilon 343 = 8.08 \times 10^3\ M^{-1}cm^{-1}$) after reduction with 3% TCEP (Tris(2-carboxyethyl)phosphine hydrochloride, 30 mg in 1 mL of H_2O).[50-52] The amount of amine per nGO was determined to be 47.25 nmole of amine/mg of nGO and estimated as ~550 amine sites per nGO, (Figure S3).

For PEGMA and nGO conjugation, the aminated nGO and 2.64 mL of 10 mg/ml carboxyl terminated PEGMA ([nGO: PEGMA] - [1:30 w/w]) were mixed with excess amount of EDC (30 mg/ml) in 10 mM MES buffer (pH 5.2). The final 11 ml of solution was gently rotated for 2-3 days at RT. Later, the sample was purified by dialysis against water, repeated centrifugation and washing cycles. Finally, the obtained [nGO-PEGMA] was completely redispersed in 10 mM HEPES (pH 7.5) to a final concentration of 200 μg/mL. Dynamic light scattering (DLS) measurements were performed using DynaPro Titan (Wyatt technology Corporation, USA).

Adsorption and desorption of DNA molecules on nGO-PEGMA. For the DNA detection studies, FAM labeled antisense DNA molecule (P1) was used as the probe strand. The [nGO-PEGMA]-P1 and nGO-P1 complexes were prepared by assembling 5 μg/mL of [nGO-PEGMA] and nGO with 20 nM P1 in 25 mM HEPES buffer (100 mM NaCl, 1 mM $MgCl_2$, pH 7.5) at 25 °C. The Fluorescence measurements (λ_{Ex}= 495 nm, λ_{Em}= 518 nm) were performed using the Fluorolog-3 spectrofluorometer (Horiba Jobin-Yvon, Inc.) equipped with a temperature controller and its software. Briefly, 20 nM P1 was prepared by diluting 1 mM stock solution in HEPES buffer immediately before each experiment. Later, 50 μL of nGO or [nGO-PEGMA] stock solutions (200 μg/mL) was added into 2 mL of 20 nM P1 solution. While, the nGO resulted in the quenching of fluorescence intensity immediately after the addition, the [nGO-PEGMA] quenching over 90 min. At the end of the incubation time, both the [nGO-PEGMA] and nGO were quenched the fluorescence ~90%. The fluorescence recovery studies were performed by addition of 8 μL of 10 μM (final 40 nM) complementary (C1) and non-complementary (nC1) into 2 mL nGO-P1 or [nGO-PEGMA]-P1 solutions. The fluorescence intensities were monitored for 150 min at 25 and 45 °C for each DNA molecule. Fluorescence recovery studies were also performed at 25, 32, 36, 39, 42, 45 and 48 °C in order to monitor the

response of the [nGO-PEGMA]-P1 to various temperatures below and above the LCST of the polymer. For regeneration studies the experiments were first performed at 25 or 45 °C, respectively. After the biodetection was over the nGO-PEGMA was reloaded with 20 nM P1 solution. The regenerated [nGO-PEGMA]-P1 was used again for the detection of 40 nM of C1 at 45 or 25 °C, respectively.

Thrombin Detection. For thrombin detection studies, 50 μL of 10 μM FAM-labeled thrombin aptamer and 300 μL of 200 μg/mL [nGO-PEGMA] solutions were incubated with 1650 μL of Tris buffer (25 mM Tris, 150 mM NaCl, 25 mM KCl, pH 7.5) at 25 °C. Resulting stock mixture was diluted 5 times in buffer to a final concentration of 50 nM of thrombin aptamer and 6 μg/mL of [nGO-PEGMA]. The fluorescence studies (λ_{Ex}= 495 nm, λ_{Em}= 518 nm) were performed with 100, 50, 20, 10 and 5 nM of final thrombin concentrations at 25 and 45 °C. The selectivity studies were carried out with 100 nM of bovine serum albumin (BSA), streptavidin (STA) and thrombin using Synergy™ H1 Microplate reader.

Adenosine Detection. For adenosine detection studies, 50 nM of FAM-labeled adenosine aptamer and 6 μg/mL of [nGO-PEGMA] were incubated in 25 mM HEPES buffer (100 mM NaCl, 1 mM $MgCl_2$, pH 7.5). The fluorescence measurements were performed with 2000, 1000, 500, 200, 100 and 50 μM of adenosine (A) using Synergy™ H1 Microplate reader, (λ_{Ex}= 495 nm, λ_{Em}= 518 nm). The selectivity studies were performed with 1 mM of adenosine (A), inosine (I), guanosine (G), cytidine (C), uridine (U) and thymine (T).

***miR*-10b detection.** 50 nM of anti-sense miR-10b DNA sequence and 6 μg/mL of [nGO-PEGMA] were incubated in 25 mM HEPES buffer (100 mM NaCl, 1 mM $MgCl_2$, pH 7.5). Fluorescence recovery studies were performed with 60, 40, 20, 10 and 5 nM of *miR*-10b at 25 and 45 °C using Synergy™ H1 Microplate reader.

Results and Discussion

We first studied the temperature-controlled detection of a short DNA molecule using our thermo-responsive nano-device. Fluorescently labeled antisense oligonucleotide (P1) was first adsorbed on the nGO-PEGMA surface during the open configuration at 25 °C. After the adsorption of the FAM labeled probe strands was established on the surface, the detection was performed at the closed (45 °C) and open configurations (25 °C), respectively. The mechanism of the detection is schematically presented in Figure 1a. At the closed configuration, the target DNA molecule (C1) has limited access to the probe strand (P1) on the nGO surface due to strong hydrophobic-hydrophobic interaction between the PEGMA polymer and graphene surface. However at 25 °C, the polymer undergoes conformational change, becomes hydrophilic,[15] and expands to the original form, which minimizes its interaction with the hydrophobic surface of nGO. At this stage, the nGO-PEGMA opens up and the entrapped probe strands become available for recognition of the target molecule. As seen in Figure 1b, at the closed configuration, the fluorescence recovery due to recognition and hybridization of the target sequence (C1) with the probe strand (P1) was approximately 2.0 million units at the end of the kinetic study. However, when the detection was carried out at the open configuration, the fluorescence recovery was around 4.0 million units. This remarkable difference was attributed to the PEGMA polymer covering the surface of the nGO and partially trapping the probe strands on the surface at the closed configuration and uncuffing them at the open configuration. The non-complementary control strands (nC1) resulted in only insignificant recovery at both configurations.

Later, we demonstrated that the difference in the amplitude of the fluorescence recovery was due to the change in the interaction between the PEGMA polymer and nGO, but not due to the

difference in the hybridization efficiencies of the DNA molecules (P1:C1 duplex) at 25 and 45 °C. Analogous experiments were carried out with bare nGO, (Figure 2 scheme). Initially, the fluorescently labeled probe stand (P1) was adsorbed on the bare nGO surface and the complementary target recognition was performed at both 25 and 45 °C. As seen in Figure 2a, the final fluorescence recovery at both temperatures are similar with a slight difference in the recovery kinetics. On the other hand, when the target (C1) recognition experiments were performed with the nGO-PEGMA complex, the recovery yield is significantly different between two temperatures. As seen in Figure 2b, at 45 °C the recovery decreased more than 50% suggesting the closed configuration at this temperature blocks the probe strands from interacting with the target sequences. Next, in order to demonstrate that the nGO-PEGMA is as powerful and sensitive as bare nGO at the open configuration, the experiments were performed at 25 °C with both materials. We have observed that the complementary target DNA sequence (C1) resulted in very similar fluorescence recovery trends and final fluorescence intensities with both nGO-PEGMA and nGO, Figure 2c. This suggests that the PEGMA polymers on the nGO-PEGMA assembly do not decrease the detection efficiency at 25 °C and the nGO-PEGMA is fully active at the open configuration. Then, in order to demonstrate that the PEGMA polymers shield the molecular recognition between the probe and target strands above the LCST (closed configuration, OFF state), we have compared the fluorescence recovery between nGO-PEGMA and bare nGO at 45 °C. As seen in Figure 2d, the fluorescence recovery with nGO at 45 °C is at its original value, however the recovery with nGO-PEGMA is diminished dramatically.

Afterwards, we studied the activity of the nGO-PEGMA at various temperatures below and above the LCST (39 °C) value of the polymer. We have performed the detection of a target DNA strand (C1) at 25, 32, 36, 39, 42, 45 and 48 °C. Figures 3a and b show that the significantly

diminished (~50%) fluorescence recoveries were observed at 42, 45 and 48 °C. This limited detection was due to the closed configuration of the nano-device at these three temperatures. However, below the LCST of the polymer a fully active nGO-PEGMA detection system was achieved due to the open configuration of the nano-device. The fluorescence signals were also plotted as intensity versus temperature, with the obtained curve (fluorescence vs. temp) having a strong agreement with the conformational change of the PEGMA polymer, Figure 3b and S1 (transmittance and hydrodynamic size). We have also demonstrated that the nano-device can be regenerated after being used for the detection of C1 at 25 °C or 45 °C and re-used at 45 °C or 25 °C, respectively, Figure 3c.

For our further studies, we have selected to use 25 °C as the open (ON state) and 45 °C as the closed (OFF state) configuration temperatures of the nGO-PEGMA nano-assembly. The dynamic light scattering results obtained with dilute solutions of nGO-PEGMA and nGO (6 μg/mL) demonstrate that the hydrodynamic size of nGO-PEGMA changes with temperature, whereas the size of the nGO remains same (Figure S2). The results indicate that the PEGMA polymers serve as temperature sensitive materials which can be used to control the physical states of their conjugated surfaces and therefore, the activity of nGO-based biosensors.

After the characterization and performance of our temperature sensitive nGO-PEGMA nano-device was performed, we used it for the detection of other biological materials including a metabolite, miRNA, and protein using surface-adsorbed aptamers or anti-sense oligonucleotides. We demonstrated the detection of adenosine as a model system, which is a small yet important metabolite that controls numerous physiological events.[53] Detection of adenosine has been performed by fluorescence, colorimetric, magnetic or electrochemical means using an aptamer highly specific to adenosine.[51, 54-60] Here, we used a fluorescently labeled adenosine aptamer and

the nGO-PEGMA nano-device for the detection of adenosine with a thermo-switch. First, the adenosine aptamer was adsorbed on the nGO-PEGMA surface at the open configuration. After the adsorption was confirmed with the quenching of the fluorescence by nGO-PEGMA, the detection was performed at two different temperatures below and above the LCST value. As seen in Figures 4a and b, at the closed configuration the fluorescence recoveries are significantly lower than the ones at the open configuration. The detection was performed with various concentration of adenosine at both configurations. The results show that more than 60% of the release was inhibited at the closed configuration, Figures 4c and d. The absorbance spectra, obtained 180 minutes after incubation with various concentrations of adenosine, demonstrate that the activity of the nano-device can be tuned with a thermo-switch below and above the LCST of the polymer. The intensities of the fluorescence readings at the open configuration were significantly higher than the ones at the closed configuration, Figures 4c and d. The result demonstrates that a significant control over the adenosine detection can be achieved using smart polymer functionalized graphene nano-device.

Afterwards we investigated the specificity of the nGO-PEGMA and FAM-labeled adenosine aptamer assembly towards adenosine. Previous studies have demonstrated that the adenosine aptamer is highly specific to adenosine and does not show any significant binding affinity towards other nucleosides.[51, 55] Therefore, selectivity experiments were performed at both temperatures with various nucleosides or metabolites including adenosine (A), thymine (T), cytidine (C), guanosine (G), uridine (U) and inosine (I). The nGO-PEGMA system is silent towards 1 mM of each compound with a diminished activity towards adenosine at the closed configuration, (Figure 5a). However, at open configuration the system is fully activated with a dramatic fluorescence recovery only with adenosine as shown in Figure 5b. The final

fluorescence recoveries with each compound at both configurations were compared in Figure 5c. As seen the nGO-PEGMA is fully active for adenosine detection at the open configuration, but only about 40% active at the closed configuration. The results demonstrate that the nGO-PEGMA is highly specific to the adenosine and its activity can be tuned with a thermo-switch between 25 and 45 °C.

After monitoring the detection of a single nucleoside with nGO-PEGMA and aptamer complex, we aimed to detect a 22 nucleotide long miRNA (*miR*-10b), which has been considered as a tumor biomarker for metastatic breast cancer.[52, 61-65] miRNAs are aberrantly expressed in the serum and/or tumor tissues of cancer patients and referred to as oncomiRs due to their critical roles in cancer.[66] OncomiRs are very stable and are considered as novel diagnostic markers and therapeutic targets.[67] Here, we controlled the activity of a nGO-PEGMA and anti-sense oligonucleotide nano-assembly for the detection of *miR*-10b. Similar to the strategies described above, the fluorescently labeled antisense oligonucleotides were adsorbed on the nGO-PEGMA surface at the open configuration. The detection of *miR*-10b relies on the hybridization of *miR*-10b to complementary fluorophore labeled DNA probe strands on nGO-PEGMA. The hybridization (miRNA/DNA hybrid) results in desorption of the probe DNA strand from the nGO-PEGMA surface, resulting in a recovery in the fluorescence. As seen in the fluorescence recoveries (Figures 6a and b), during the closed configuration the *miR*-10b detection is significantly diminished (~60%) when compared to the open configuration. The fluorescence recovery observed at 10 nM of *miR*-10b at the open configuration is equivalent to the recovery observed with 60 nM of *miR*-10b at the closed configuration, Figures 6c and d. The fluorescence spectra, at the end of the 220 minutes of incubation with various concentrations of *miR*-10b at the OFF and ON states, demonstrate that the activity of the nano-device depends strongly on the

LCST of the conjugated PEGMA molecules. The intensities of the fluorescence readings were higher in the open configuration than the closed configuration, Figures 6c and d. The detection was performed for different concentrations of *miR*-10b at both temperatures and a clear decrease in activity was observed at the closed configuration. Detection and silencing of oncomiRs are novel approaches for diagnosis and therapy of cancer at the molecular level. Therefore, an activatable system that could bind and knockdown the function of specific miRNAs at tissue of interest with minimized off-target effect could have a major impact on cancer theranostics.

After demonstration of a small metabolite, DNA and an oncogene detection at the ON and OFF states of our nano-device, we studied the detection of a protein as another type of biomolecule. Thrombin is a serine protease whose expression level is critical for fatal medical conditions including cerebral ischemia and stroke.[68] Thrombin has a strong binding affinity to a highly specific DNA aptamer, which has been used as a model system for validating the binding performance of aptamers towards proteins.[50, 67, 69] Here, we controlled the activity of a nGO-PEGMA and fluorophore labeled thrombin aptamer nano-assembly for the detection of thrombin. The aptamer was first complexed with the nGO-PEGMA at ON state. After quenching of the fluorescence was observed upon adsorption of the aptamer on the nGO-PEGMA surface, detection of various concentrations of thrombin was performed at the ON and OFF states of the nano-assembly. As shown in Figure 7a and 7c, the nGO-PEGMA and aptamer complex has a very slow and diminished response towards thrombin at the OFF state. However, the detection is dramatically faster and the fluorescence recovery is significantly higher at the ON state (Figure 7b and 7d). Then, we monitored the sensitivity of the system to thrombin at the ON and OFF states at various concentrations. As seen in Figure 7e, as the thrombin concentration increases, the difference between fluorescence signals at both configurations becomes more dramatic. We

have observed that the fluorescence signal with 10 nM thrombin at the ON state is higher than the signal with 100 nM thrombin at the OFF state.

Next, the selectivity of the system was demonstrated below and above the LCST of the PEGMA. Streptavidin (STA) and bovine serum albumin (BSA) were used as control proteins for the thrombin specific aptamer. In Figure 7f, the fluorescence recoveries with STA and BSA at both temperatures are at background levels and significantly lower than thrombin induced fluorescence recovery. Similar to the other biomolecule detection schemes, the results show that the detection was diminished more than ~80% at the closed configuration. The results overall show that the nGO-PEGMA and aptamer nano-assembly is highly specific to thrombin and its activity can be tuned with temperatures above and below the LCST.

Conclusion

In summary, we have successfully demonstrated a robust strategy for engineering smart thermo-responsive nano-devices composed of PEGMA polymer and graphene oxide. The activatable nano-device is used for the detection of oligonucleotides, a small metabolic compound and protein. In this system, the PEGMA plays a vital role in entrapping and releasing probe strands in a controlled manner. The nGO-PEGMA showed a strong retention strength when the temperature is above the LCST value and almost no retention when below. Fluorescence studies showed two distinctive release kinetics with temperatures above and below the LCST value. The prepared thermo-responsive material is able to entrap the FAM labeled probe DNA strands or aptamers with excellent loading efficiency. The nGO on the surface serves as a fluorescence quencher and template for the probe DNA strands, whereas the PEGMA molecules serve as a shield over DNA molecules which could be switched on and off with a change in temperature.

We have controlled the activity of the nano-device for the detection of four different biomolecule types - sequence specific DNA, *miR*-10b, thrombin and adenosine. The activity of our functional system can be decreased by ~80% with a thermo-switch. Furthermore, our approach could be generalized for other aptamer or DNAzyme based sensing strategies for the detection of environmentally or biologically important compounds. Since nGO has been used for various cancer theranostics, in the long run, this approach can be extended to advanced biomedical applications after a total control over the activity of the nano-assembly is achieved. Particularly, releasing encapsulated therapeutic and diagnostic materials at diseased tissue with external stimuli could have powerful implications for controllable targeted gene/drug delivery approaches.

Supporting Information

Additional graphical data and images are provided in the supporting information.

Acknowledgements. We acknowledge the Ministry of National Education, Republic of Turkey, for financial support to Mustafa Balcioglu with full fellowship during his doctoral studies. This work was supported by the SUNY Albany Start-Up Funds.

References

1. Carter, K. A.; Shao, S.; Hoopes, M. I.; Luo, D.; Ahsan, B.; Grigoryants, V. M.; Song, W.; Huang, H.; Zhang, G.; Pandey, R. K.; Geng, J.; Pfeifer, B. A.; Scholes, C. P.; Ortega, J.; Karttunen, M.; Lovell, J. F. Porphyrin-Phospholipid Liposomes Permeabilized by near-Infrared Light. *Nat. Commun.* **2014,** *5*, 3546, 10.1038/ncomms4546.

2. Yavuz, M. S.; Cheng, Y.; Chen, J.; Cobley, C. M.; Zhang, Q.; Rycenga, M.; Xie, J.; Kim, C.; Song, K. H.; Schwartz, A. G.; Wang, L. V.; Xia, Y. Gold Nanocages Covered by Smart Polymers for Controlled Release with near-Infrared Light. *Nat. Mater.* **2009,** *8*, 935-939, 10.1038/nmat2564.

3. Huang, H.; Song, W.; Chen, G.; Reynard, J. M.; Ohulchanskyy, T. Y.; Prasad, P. N.; Bright, F. V.; Lovell, J. F. Pd-Porphyrin-Cross-Linked Implantable Hydrogels with Oxygen-Responsive Phosphorescence. *Adv. Healthc. Mater.* **2014,** *3*, 891-896, 10.1002/adhm.201300483.

4. Roy, D.; Brooks, W. L.; Sumerlin, B. S. New Directions in Thermoresponsive Polymers. *Chem. Soc. Rev.* **2013,** *42*, 7214-7243, 10.1039/c3cs35499g.

5. Hamner, K. L.; Alexander, C. M.; Coopersmith, K.; Reishofer, D.; Provenza, C.; Maye, M. M. Using Temperature-Sensitive Smart Polymers to Regulate DNA-Mediated Nanoassembly and Encoded Nanocarrier Drug Release. *ACS Nano* **2013,** *7*, 7011-7020, 10.1021/nn402214e.

6. Acar, H.; Genc, R.; Urel, M.; Erkal, T. S.; Dana, A.; Guler, M. O. Self-Assembled Peptide Nanofiber Templated One-Dimensional Gold Nanostructures Exhibiting Resistive Switching. *Langmuir* **2012,** *28*, 16347-16354, 10.1021/la3035215.

7. Sulek, S.; Mammadov, B.; Mahcicek, D. I.; Sozeri, H.; Atalar, E.; Tekinay, A. B.; Guler, M. O. Peptide Functionalized Superparamagnetic Iron Oxide Nanoparticles as Mri Contrast Agents. *J. Mater. Chem.* **2011,** *21*, 15157-15162, Doi 10.1039/C1jm11387a.

8. Mieszawska, A. J.; Mulder, W. J.; Fayad, Z. A.; Cormode, D. P. Multifunctional Gold Nanoparticles for Diagnosis and Therapy of Disease. *Mol. Pharm.* **2013,** *10*, 831-847, 10.1021/mp3005885.

9. Allijn, I. E.; Leong, W.; Tang, J.; Gianella, A.; Mieszawska, A. J.; Fay, F.; Ma, G.; Russell, S.; Callo, C. B.; Gordon, R. E.; Korkmaz, E.; Post, J. A.; Zhao, Y.; Gerritsen, H. C.; Thran, A.; Proksa, R.; Daerr, H.; Storm, G.; Fuster, V.; Fisher, E. A.; Fayad, Z. A.; Mulder, W. J.; Cormode, D. P. Gold Nanocrystal Labeling Allows Low-Density Lipoprotein Imaging from the Subcellular to Macroscopic Level. *ACS Nano* **2013,** *7*, 9761-9770, 10.1021/nn403258w.

10. Alexander, C. M.; Hamner, K. L.; Maye, M. M.; Dabrowiak, J. C. Multifunctional DNA-Gold Nanoparticles for Targeted Doxorubicin Delivery. *Bioconjugate Chem.* **2014**, 10.1021/bc500136r.

11. Hamner, K. L.; Maye, M. M. Thermal Aggregation Properties of Nanoparticles Modified with Temperature Sensitive Copolymers. *Langmuir* **2013,** *29*, 15217-15223, 10.1021/la4037887.

12. Pan, Y.; Bao, H.; Sahoo, N. G.; Wu, T.; Li, L. Water-Soluble Poly(N-Isopropylacrylamide)–Graphene Sheets Synthesized Via Click Chemistry for Drug Delivery. *Adv. Funct. Mater.* **2011,** *21*, 2754-2763, 10.1002/adfm.201100078.

13. Ward, M. A.; Georgiou, T. K. Thermoresponsive Polymers for Biomedical Applications. *Polymers* **2011,** *3*, 1215-1242, Doi 10.3390/Polym3031215.

14. Lutz, J. F.; Hoth, A. Preparation of Ideal Peg Analogues with a Tunable Thermosensitivity by Controlled Radical Copolymerization of 2-(2-Methoxyethoxy)Ethyl Methacrylate and Oligo(Ethylene Glycol) Methacrylate. *Macromolecules* **2006,** *39*, 893-896, Doi 10.1021/Ma0517042.

15. Ulasan, M.; Yavuz, E.; Bagriacik, E. U.; Cengeloglu, Y.; Yavuz, M. S. Biocompatible Thermoresponsive Pegma Nanoparticles Crosslinked with Cleavable Disulfide-Based Crosslinker for Dual Drug Release. *J. Biomed. Mater. Res. A* **2014**, 10.1002/jbm.a.35146.

16. Lian, X.; Jin, J.; Tian, J.; Zhao, H. Thermoresponsive Nanohydrogels Cross-Linked by Gold Nanoparticles. *ACS Appl. Mater. Interfaces* **2010,** *2*, 2261-2268, 10.1021/am1003156.

17. Fan, X.; Jiao, G.; Zhao, W.; Jin, P.; Li, X. Magnetic Fe3o4-Graphene Composites as Targeted Drug Nanocarriers for Ph-Activated Release. *Nanoscale* **2013,** *5*, 1143-1152, 10.1039/c2nr33158f.

18. Bak, J. M.; Lee, T.; Seo, E.; Lee, Y.; Jeong, H. M.; Kim, B. S.; Lee, H. I. Thermoresponsive Graphene Nanosheets by Functionalization with Polymer Brushes. *Polymer* **2012,** *53*, 316-323, DOI 10.1016/j.polymer.2011.11.057.

19. Lee, S. Y.; Kim, S. H.; Kim, S. M.; Lee, H.; Lee, G.; Park, S. Y. Tunable and Selective Detection of Cancer Cells Using a Betainized Zwitterionic Polymer with Bodipy and Graphene Oxide. *New J. Chem.* **2014,** *38*, 2225-2228, Doi 10.1039/C3nj01641b.

20. Mosaiab, T.; In, I.; Park, S. Y. Temperature and Ph-Tunable Fluorescence Nanoplatform with Graphene Oxide and Bodipy-Conjugated Polymer for Cell Imaging and Therapy. *Macromol. Rapid. Commun.* **2013,** *34*, 1408-1415, 10.1002/marc.201300413.

21. Wen, H.; Dong, C.; Dong, H.; Shen, A.; Xia, W.; Cai, X.; Song, Y.; Li, X.; Li, Y.; Shi, D. Engineered Redox-Responsive Peg Detachment Mechanism in Pegylated Nano-Graphene Oxide for Intracellular Drug Delivery. *Small* **2012,** *8*, 760-769, 10.1002/smll.201101613.

22. Magnusson, J. P.; Khan, A.; Pasparakis, G.; Saeed, A. O.; Wang, W.; Alexander, C. Ion-Sensitive "Isothermal" Responsive Polymers Prepared in Water. *J. Am. Chem.Soc.* **2008,** *130*, 10852-10853, 10.1021/ja802609r.

23. Xulu, P. M.; Filipcsei, G.; Zrinyi, M. Preparation and Responsive Properties of Magnetically Soft Poly(N-Isopropylacrylamide) Gels. *Macromolecules* **2000,** *33*, 1716-1719, Doi 10.1021/Ma990967r.

24. Czaun, M.; Hevesi, L.; Takafuji, M.; Ihara, H. A Novel Approach to Magneto-Responsive Polymeric Gels Assisted by Iron Nanoparticles as Nano Cross-Linkers. *Chem. Commun. (Camb)* **2008**, 2124-2126, 10.1039/b717721f.

25. Keng, P. Y.; Shim, I.; Korth, B. D.; Douglas, J. F.; Pyun, J. Synthesis and Self-Assembly of Polymer-Coated Ferromagnetic Nanoparticles. *ACS Nano* **2007,** *1*, 279-292, 10.1021/nn7001213.

26. Szabo, D.; Szeghy, G.; Zrinyi, M. Shape Transition of Magnetic Field Sensitive Polymer Gels. *Macromolecules* **1998,** *31*, 6541-6548, Doi 10.1021/Ma980284w.

27. Xia, H.; Xu, Y.; Yang, G.; Jiang, H.; Zou, G.; Zhang, Q. A Reversible Multi-Stimuli-Responsive Fluorescence Probe and the Design for Combinational Logic Gate Operations. *Macromol. Rapid. Commun.* **2014,** *35*, 303-308, 10.1002/marc.201300829.

28. Jochum, F. D.; zur Borg, L.; Roth, P. J.; Theato, P. Thermo- and Light-Responsive Polymers Containing Photoswitchable Azobenzene End Groups. *Macromolecules* **2009,** *42*, 7854-7862, Doi 10.1021/Ma901295f.

29. Jochum, F. D.; Theato, P. Temperature and Light Sensitive Copolymers Containing Azobenzene Moieties Prepared Via a Polymer Analogous Reaction. *Polymer* **2009,** *50*, 3079-3085, DOI 10.1016/j.polymer.2009.05.041.

30. Jiang, J.; Tong, X.; Zhao, Y. A New Design for Light-Breakable Polymer Micelles. *J. Am. Chem. Soc.* **2005,** *127*, 8290-8291, 10.1021/ja0521019.

31. Lovell, J. F.; Liu, T. W.; Chen, J.; Zheng, G. Activatable Photosensitizers for Imaging and Therapy. *Chem. Rev.* **2010,** *110*, 2839-2857, 10.1021/cr900236h.

32. Zhang, J.; Song, L.; Zhang, Z.; Chen, N.; Qu, L. Environmentally Responsive Graphene Systems. *Small* **2014,** *10*, 2151-2164, 10.1002/smll.201303080.

33. Lutz, J. F.; Weichenhan, K.; Akdemir, O.; Hoth, A. About the Phase Transitions in Aqueous Solutions of Thermoresponsive Copolymers and Hydrogels Based on 2-(2-Methoxyethoxy)Ethyl Methacrylate and Oligo(Ethylene Glycol) Methacrylate. *Macromolecules* **2007,** *40*, 2503-2508, Doi 10.1021/Ma062925q.

34. Lutz, J. F. Thermo-Switchable Materials Prepared Using the Oegma-Platform. *Adv. Mater.* **2011,** *23*, 2237-2243, DOI 10.1002/adma.201100597.

35. Dreyer, D. R.; Park, S.; Bielawski, C. W.; Ruoff, R. S. The Chemistry of Graphene Oxide. *Chem. Soc. Rev.* **2010,** *39*, 228-240, 10.1039/b917103g.

36. Allen, M. J.; Tung, V. C.; Kaner, R. B. Honeycomb Carbon: A Review of Graphene. *Chem. Rev.* **2010,** *110*, 132-145, 10.1021/cr900070d.

37. Rana, M.; Balcioglu, M.; Robertson, N.; Yigit, M. V. Nano-Graphene Oxide as a Novel Platform for Monitoring the Effect of Lna Modification on Nucleic Acid Interactions. *Analyst* **2014,** *139*, 714-720, 10.1039/c3an02066e.

38. Balcioglu, M.; Rana, M.; Robertson, N.; Yigit, M. V. DNA-Length-Dependent Quenching of Fluorescently Labeled Iron Oxide Nanoparticles with Gold, Graphene Oxide and Mos2 Nanostructures. *ACS Appl. Mater. Interfaces* **2014,** *6*, 12100-12110, 10.1021/am503553h.

39. Balcioglu, M.; Rana, M.; Yigit, M. V. Doxorubicin Loading on Graphene Oxide, Iron Oxide and Gold Nanoparticle Hybrid. *J. Mater. Chem. B* **2013**, 10.1039/C3TB20992J.

40. Hizir, M. S.; Balcioglu, M.; Rana, M.; Robertson, N. M.; Yigit, M. V. Simultaneous Detection of Circulating Oncomirs from Body Fluids for Prostate Cancer Staging Using Nanographene Oxide. *ACS Appl. Mater. Interfaces* **2014,** *6*, 14772–14778, 10.1021/am504190a.

41. Liu, J. Adsorption of DNA onto Gold Nanoparticles and Graphene Oxide: Surface Science and Applications. *Phys. Chem. Chem. Phys.* **2012,** *14*, 10485-10496, 10.1039/c2cp41186e.

42. Wu, M.; Kempaiah, R.; Huang, P. J.; Maheshwari, V.; Liu, J. Adsorption and Desorption of DNA on Graphene Oxide Studied by Fluorescently Labeled Oligonucleotides. *Langmuir* **2011**, 10.1021/la1037926.

43. Liu, B.; Sun, Z.; Zhang, X.; Liu, J. Mechanisms of DNA Sensing on Graphene Oxide. *Anal. Chem.* **2013,** *85*, 7987-7993, 10.1021/ac401845p.

44. Huang, P. J.; Liu, J. DNA-Length-Dependent Fluorescence Signaling on Graphene Oxide Surface. *Small* **2012,** *8*, 977-983, 10.1002/smll.201102156.

45. Huang, P. J.; Liu, J. Molecular Beacon Lighting up on Graphene Oxide. *Anal. Chem.* **2012,** *84*, 4192-4198, 10.1021/ac300778s.

46. Yang, K.; Feng, L.; Hong, H.; Cai, W.; Liu, Z. Preparation and Functionalization of Graphene Nanocomposites for Biomedical Applications. *Nat. Protoc.* **2013,** *8*, 2392-2403, 10.1038/nprot.2013.146.

47. Layek, R. K.; Nandi, A. K. A Review on Synthesis and Properties of Polymer Functionalized Graphene. *Polymer* **2013,** *54*, 5087-5103, DOI 10.1016/j.polymer.2013.06.027.

48. Jung, Y. K.; Lee, T.; Shin, E.; Kim, B. S. Highly Tunable Aptasensing Microarrays with Graphene Oxide Multilayers. *Sci. Rep.* **2013,** *3*, 3367, 10.1038/srep03367.

49. Wei, Q.; Nagi, R.; Sadeghi, K.; Feng, S.; Yan, E.; Ki, S. J.; Caire, R.; Tseng, D.; Ozcan, A. Detection and Spatial Mapping of Mercury Contamination in Water Samples Using a Smart-Phone. *ACS Nano* **2014,** *8*, 1121-1129, 10.1021/nn406571t.

50. Yigit, M. V.; Mazumdar, D.; Lu, Y. Mri Detection of Thrombin with Aptamer Functionalized Superparamagnetic Iron Oxide Nanoparticles. *Bioconjugate Chem.* **2008,** *19*, 412-417, 10.1021/bc7003928.

51. Yigit, M. V.; Mazumdar, D.; Kim, H. K.; Lee, J. H.; Odintsov, B.; Lu, Y. Smart "Turn-on" Magnetic Resonance Contrast Agents Based on Aptamer-Functionalized Superparamagnetic Iron Oxide Nanoparticles. *Chembiochem* **2007,** *8*, 1675-1678, 10.1002/cbic.200700323.

52. Yigit, M. V.; Ghosh, S. K.; Kumar, M.; Petkova, V.; Kavishwar, A.; Moore, A.; Medarova, Z. Context-Dependent Differences in Mir-10b Breast Oncogenesis Can Be Targeted for the Prevention and Arrest of Lymph Node Metastasis. *Oncogene* **2013,** *32*, 1530-1538, 10.1038/onc.2012.173.

53. Hasko, G.; Linden, J.; Cronstein, B.; Pacher, P. Adenosine Receptors: Therapeutic Aspects for Inflammatory and Immune Diseases. *Nat. Rev. Drug Discov.* **2008,** *7*, 759-770, 10.1038/nrd2638.

54. Huizenga, D. E.; Szostak, J. W. A DNA Aptamer That Binds Adenosine and Atp. *Biochemistry* **1995,** *34*, 656-665, 10.1021/Bi00002a033.

55. Liu, J.; Lu, Y. Fast Colorimetric Sensing of Adenosine and Cocaine Based on a General Sensor Design Involving Aptamers and Nanoparticles. *Angew. Chem. Int. Ed .Engl.* **2005,** *45*, 90-94, 10.1002/anie.200502589.

56. Huang, P. J.; Liu, J. Flow Cytometry-Assisted Detection of Adenosine in Serum with an Immobilized Aptamer Sensor. *Anal. Chem.* **2010,** *82*, 4020-4026, 10.1021/ac9028505.

57. Kim, J.; Kim, I. Y.; Choi, M. S.; Wu, Q. Label-Free Electrochemical Detection of Adenosine Based on Electron Transfer from Guanine Bases in an Adenosine-Sensitive Aptamer. *Chem. Commun. (Camb)* **2009**, 4747-4749, 10.1039/b908344h.

58. Helwa, Y.; Dave, N.; Froidevaux, R.; Samadi, A.; Liu, J. Aptamer-Functionalized Hydrogel Microparticles for Fast Visual Detection of Mercury(Ii) and Adenosine. *ACS Appl. Mater. Interfaces* **2012,** *4*, 2228-2233, 10.1021/am300241j.

59. Li, L. L.; Ge, P.; Selvin, P. R.; Lu, Y. Direct Detection of Adenosine in Undiluted Serum Using a Luminescent Aptamer Sensor Attached to a Terbium Complex. *Anal. Chem.* **2012,** *84*, 7852-7856, 10.1021/ac302167d.

60. Liu, J.; Lu, Y. Adenosine-Dependent Assembly of Aptazyme-Functionalized Gold Nanoparticles and Its Application as a Colorimetric Biosensor. *Anal. Chem.* **2004,** *76*, 1627-1632, 10.1021/ac0351769.

61. Rana, M.; Balcioglu, M.; Yigit, M. V. Locked Nucleic Acid-Modified Antisense Mir-10b Oligonucleotides Form Stable Duplexes on Gold Nanoparticles. *BioNanoScience* **2014**, 10.1007/s12668-014-0130-0.

62. Robertson, N. M.; Yigit, M. V. The Role of Microrna in Resistanceto Breast Cancer Therapy. *WIREs RNA*, 10.1002/wrna.1248.

63. Ma, L.; Reinhardt, F.; Pan, E.; Soutschek, J.; Bhat, B.; Marcusson, E. G.; Teruya-Feldstein, J.; Bell, G. W.; Weinberg, R. A. Therapeutic Silencing of Mir-10b Inhibits Metastasis in a Mouse Mammary Tumor Model. *Nat. Biotechnol.* **2010,** *28*, 341-347, 10.1038/nbt.1618.

64. Ma, L.; Teruya-Feldstein, J.; Weinberg, R. A. Tumour Invasion and Metastasis Initiated by Microrna-10b in Breast Cancer. *Nature* **2007,** *449*, 682,

65. Ma, L. Role of Mir-10b in Breast Cancer Metastasis. *Breast Cancer Res.* **2010,** *12*, 210, 10.1186/bcr2720.

66. Esquela-Kerscher, A.; Slack, F. J. Oncomirs - Micrornas with a Role in Cancer. *Nat. Rev. Cancer* **2006,** *6*, 259-269, 10.1038/nrc1840.

67. Mitchell, P. S.; Parkin, R. K.; Kroh, E. M.; Fritz, B. R.; Wyman, S. K.; Pogosova-Agadjanyan, E. L.; Peterson, A.; Noteboom, J.; O'Briant, K. C.; Allen, A.; Lin, D. W.; Urban, N.; Drescher, C. W.; Knudsen, B. S.; Stirewalt, D. L.; Gentleman, R.; Vessella, R. L.; Nelson, P. S.; Martin, D. B.; Tewari, M. Circulating Micrornas as Stable Blood-Based Markers for Cancer Detection. *Proc. Natl. Acad. Sci. USA* **2008,** *105*, 10513-10518, 10.1073/pnas.0804549105.

68. Uppal, R.; Caravan, P. Targeted Probes for Cardiovascular Mri. *Future Med. Chem.* **2010,** *2*, 451-470, 10.4155/FMC.09.154.

69. Wang, L.; Zhu, J.; Han, L.; Jin, L.; Zhu, C.; Wang, E.; Dong, S. Graphene-Based Aptamer Logic Gates and Their Application to Multiplex Detection. *ACS Nano* **2012,** *6*, 6659-6666, 10.1021/nn300997f.

Figures.

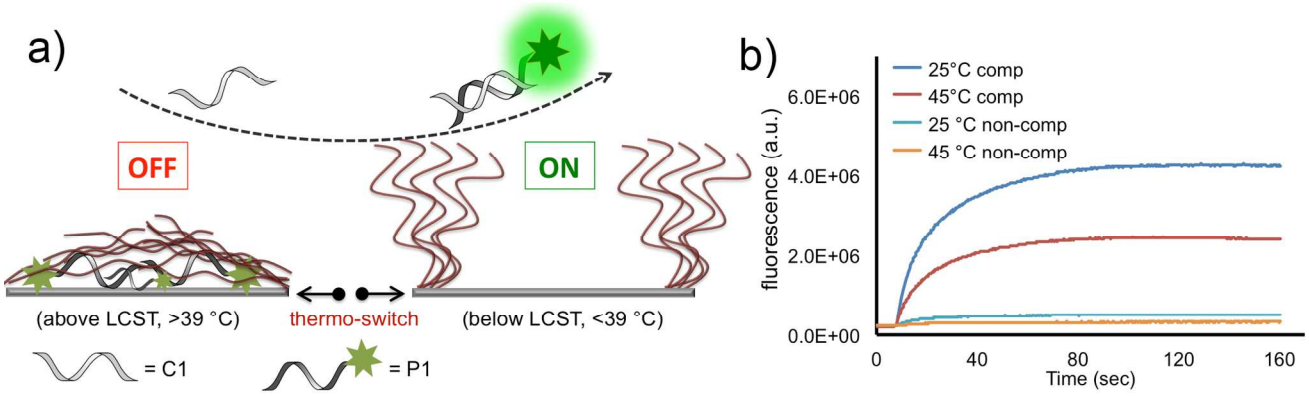

Figure 1. (a) Schematic representation of the thermo-responsive smart nGO-PEGMA and fluorophore labeled probe DNA (P1) nano-device for the detection of a sequence-specific DNA molecule (C1). (b) Fluorescence recovery with complementary and non-complementary DNA molecules at the closed (45 °C) and open configurations (25 °C), indicates a strong dependence on the complementarity and the configuration of the PEGMA.

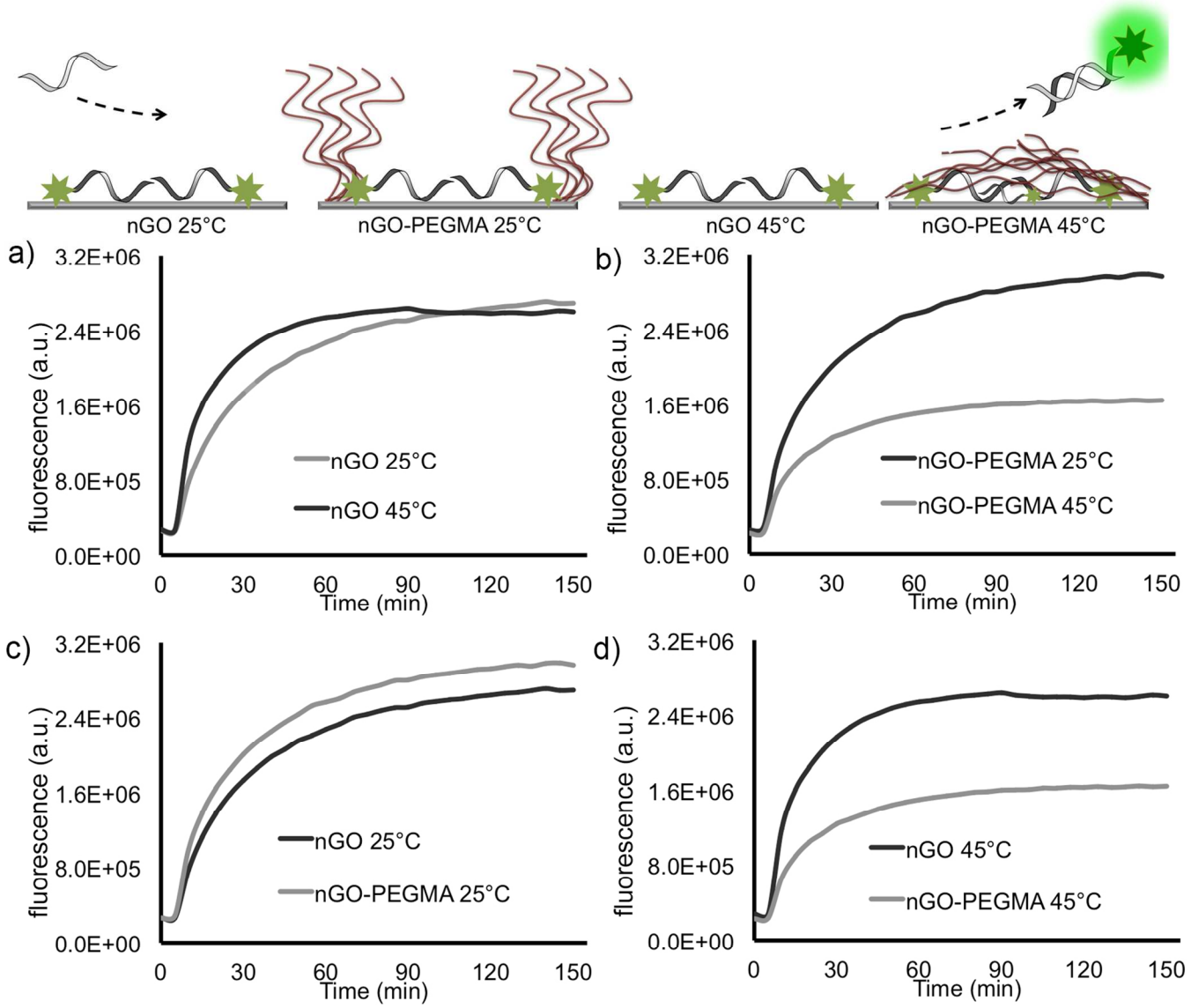

Figure 2. Fluorescence recoveries in the presence of sequence-specific DNA (C1) molecules using probe stand (P1) adsorbed (a) nGO at 25 and 45 °C ,(b) nGO-PEGMA at 25 (ON state) and 45 °C (OFF state), (c) nGO and nGO-PEGMA at 25 °C and, (d) nGO and nGO-PEGMA at 45 °C.

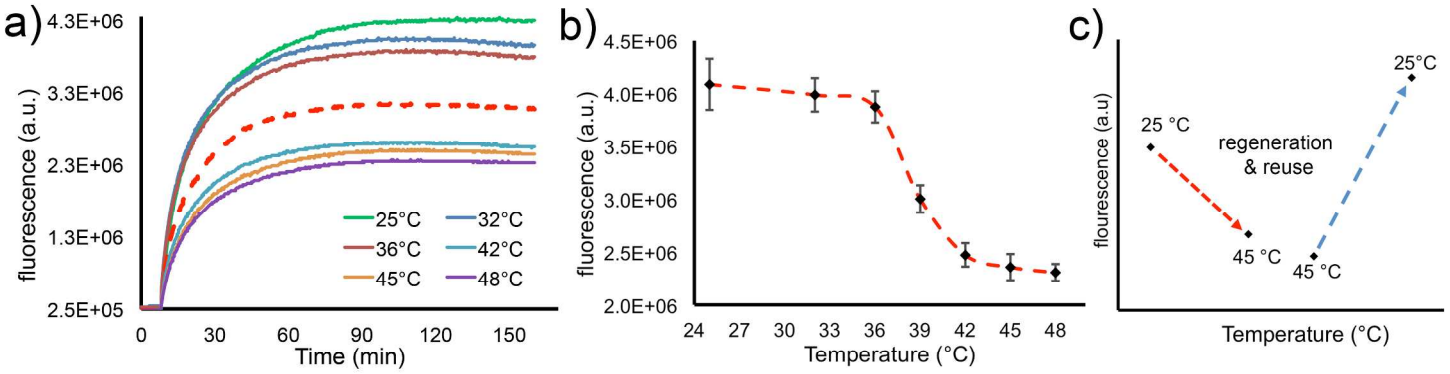

Figure 3. Controlling the activity of the nGO-PEGMA and probe DNA (P1) nano-device with a thermo-switch for the detection of a sequence-specific DNA molecule. The fluorescence (a) recoveries over time show strong dependence on the LCST of the polymer. (b) The fluorescence intensities at seven different temperatures indicate complete activity below the LCST and inhibited activity above the LCST. (c) The nano-device can be used, regenerated and reused at 25 °C and 45 °C or 45 °C and 25 °C.

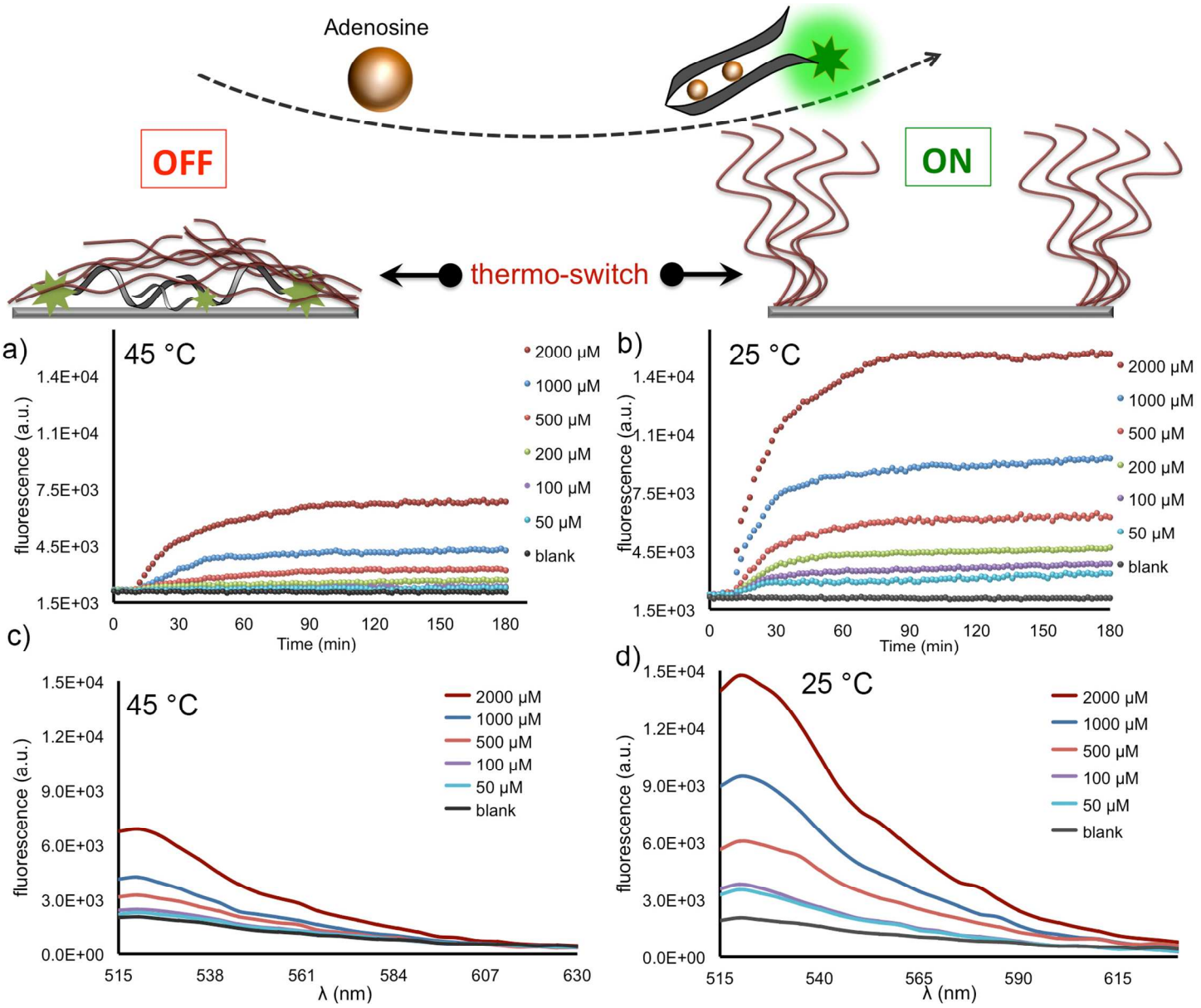

Figure 4. Activation of the smart nGO-PEGMA and aptamer nano-device for the detection of adenosine with a thermo-switch. Fluorescence recoveries with various concentrations of adenosine at the (a) OFF state at 45 °C and (b) ON state at 25 °C. The fluorescence spectra at the end of the 180 minutes of incubation with various concentrations of adenosine at (c) OFF state and (d) ON state.

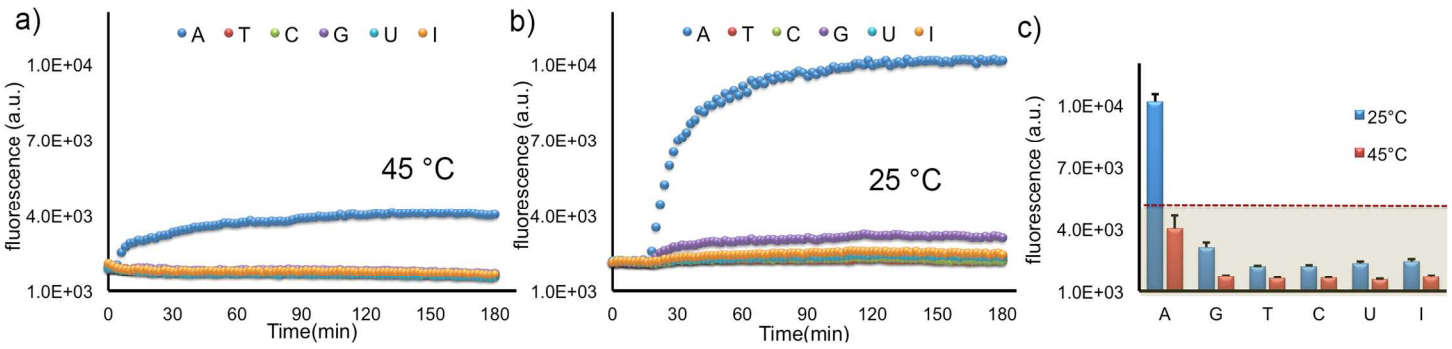

Figure 5. Specificity of nGO-PEGMA and adenosine aptamer towards adenosine is determined by incubation with 1 mM of adenosine (A), thymine (T), cytidine (C), guanosine (G), uridine (U) and inosine (I) at the (a) OFF state and (b) ON state. (c) The final fluorescence intensities after 180 minutes of incubation shows strong specificity and temperature dependence.

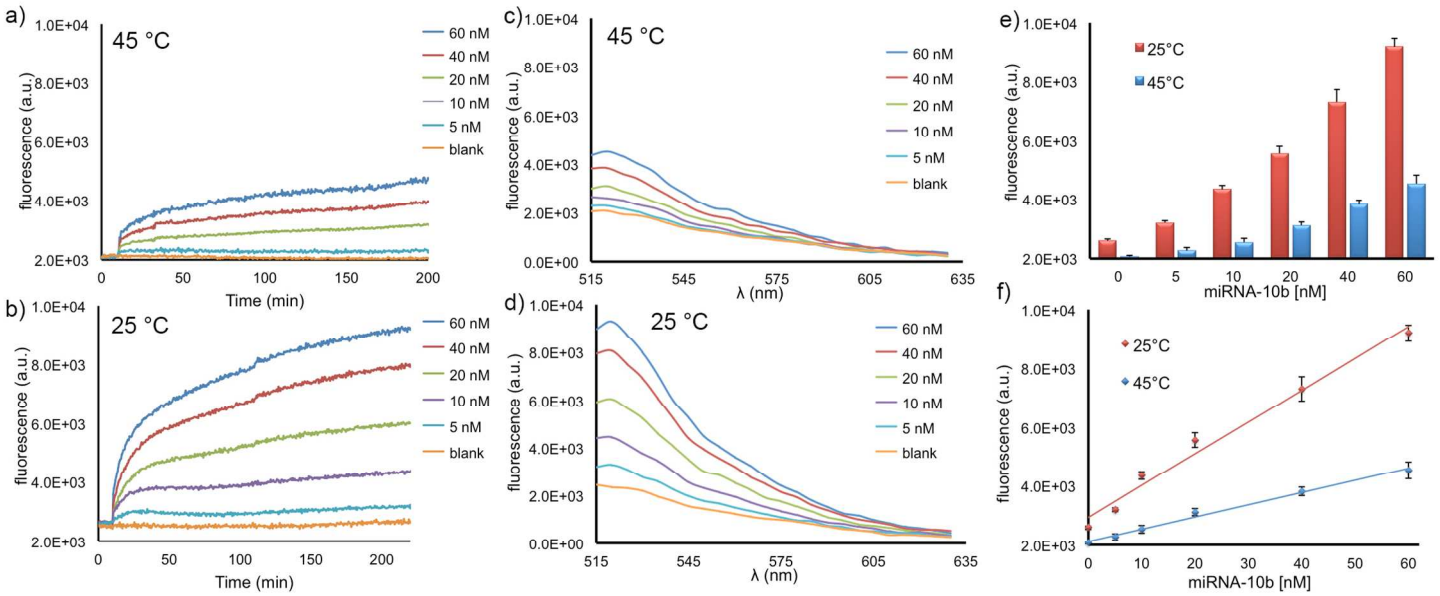

Figure 6. Activation of the smart nGO-PEGMA and FAM labeled anti-sense *miR*-10b assembly for the detection of *miR*-10b with a thermo-switch. Fluorescence recoveries with various concentrations of *miR*-10b at the (a) OFF state and (b) ON state. The fluorescence spectra at the end of the 220 minutes of incubation with various concentrations of *miR*-10b at (c) OFF state and (d) ON state. (e) and (f) The final fluorescence signals indicate that the activity of the nano-assembly can be controlled with the thermo-switch at 39 °C for *miR*-10b detection.

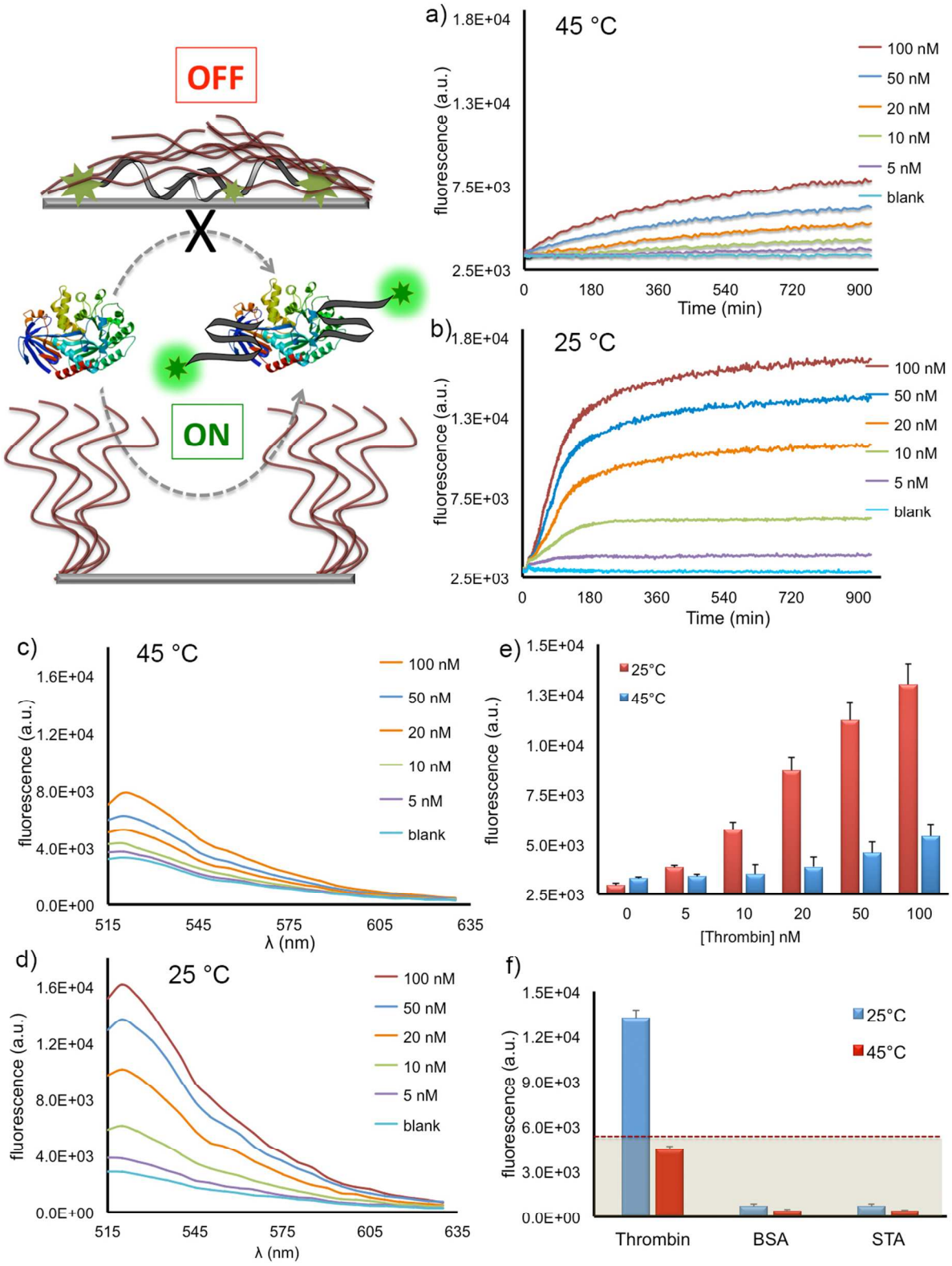

Figure 7. Activation of the smart nGO-PEGMA and FAM labeled thrombin aptamer assembly for the detection of thrombin with a thermo-switch. Fluorescence recoveries with various concentrations of thrombin at the (a) closed and (b) open configurations. The fluorescence spectra at various concentrations of thrombin at (c) 45 and (d) 25 °C. The final fluorescence signals at minute 180 indicate that (e) the activity of the nano-assembly can be tuned with the thermo-switch at 39°C and, (f) the system in highly specific to thrombin.

Table of Content Figure: